Cretaceous Research 114 (2020) 104502

Contents lists available at ScienceDirect

Cretaceous Research

journal homepage: www.elsevier.com/locate/CretRes

New haidomyrmecine ants (Hymenoptera: Formicidae) from mid-Cretaceous amber of northern Myanmar

John E. Lattke *, Gabriel A.R. Melo

Universidade Federal do Paraná, Departamento de Zoologia, Curitiba, PR, CEP 81531-980, Brazil

ARTICLE INFO

Article history:
Received 24 October 2019
Received in revised form
6 March 2020
Accepted in revised form 7 May 2020
Available online 27 May 2020

Keywords:
Stem-group ants
Taxonomy
Morphology
Kachin amber
Behavior

ABSTRACT

Three new species and a new genus of "hell ants" (Haidomyrmecinae) are described from Cenomanian Burmese amber. *Ceratomyrmex planus* sp. nov. is the second species formally known for the genus and obliges a revision of the generic diagnosis. It can be recognized by its smaller size, the straight and shorter club-like cephalic horn, and flattened eyes. *Haidomyrmex davidbowiei* sp. nov. has only two trigger hairs on the apex of a brief clypeal lobe dorsal to the setal patch, the first flagellomere distinctly longer than the second, amongst other characters. *Dilobops bidentata* gen. et sp. nov., is the only known ant with a bidentate projection on the frontal region. Its clypeus is posteriorly flanked by two projecting lobes. The possible relation of the cephalic and mandibular morphology with the feeding habits of Haidomyrmecinae is discussed. It is argued that not all species impaled prey with their mandibles and that honeydew collection could have formed a part of their diet. A key for identifying the species of *Haidomyrmex* is included.

1. Introduction

The Haidomyrmecinae are a stem group of ants with a fossil record spanning some 20 million years during the mid to late Cretaceous, within the period also known as the Cretaceous Terrestrial Revolution (KTR), a lapse spanning 125–80 Ma when the dominance of gymnosperm floras was down-sized from almost 100% to some 20% (Wang et al., 2016). These ants have been found in amber deposits from France, Myanmar, and Canada. Despite their extraction from relatively few deposits, fourteen species and nine genera have already been described. The first haidomyrmecine, *Haidomyrmex cerberus* Dlussky, was described from a single specimen encased in Burmese amber in 1996 and considered a specialized predator on account of its peculiar mandibular morphology and apparent trigger hairs on the head, suggesting a trap-like hunting mechanism. Recently Cao et al. (2020) have redescribed in greater detail this species using additional specimens. Bolton (2003) puts *Haidomyrmex* within its own tribe, Haidomyrmecini, in the subfamily Sphecomyrmecinae. Perrichot et al. (2008) extends the geographic distribution of these ants by describing a new genus, *Haidomyrmodes*, from French amber. Barden and Grimaldi (2012) add two additional species to the genus *Haidomyrmex*, discuss the relation between the known haidomyrmecines and propose movement of their mandibles in a vertical plane, with the possibility of prey impalement in some cases. McKellar et al. (2013) expand haidomyrmecine distribution in space and time by describing another genus, *Haidoterminus*, from Canadian amber younger than the French and Burmese ambers. Recent reviews of the species have been authored by Barden et al. (2017) and Perrichot et al. (2016), in both cases describing additional genera with more elaborate cephalic morphology than previously known haidomyrmecines. Perrichot et al. (2016) also offer reappraisals of previously described species, clearing ambiguities and describing new morphological details. Miao and Wang (2019) describe a second species of *Linguamyrmex*, a genus described by Barden et al. (2017). Most recently, Perrichot et al. (2020) describe four genera and five species as well as provide an identification key for the genera and species. They also argue for and formally propose subfamily rank for these ants. The shape of the mandibles and head in these ants, as well as their inferred predation behavior, is so unlike anything known in extant ants that it has earned them a visibility, even to the broader public, as "hell ants". In this study, we describe three new species of haidomyrmecine ants, each belonging to a different genus, including a new genus, all from inclusions in Cenomanian Kachin amber from northern Myanmar. We include images of the new species, discuss the differences and

* Corresponding author.
E-mail address: lattke@ufpr.br (J.E. Lattke).

https://doi.org/10.1016/j.cretres.2020.104502
0195-6671/

similarities of these taxa with known haidomyrmecines, and present an updated key to the species of *Haidomyrmex*. We also consider how the cephalic shape, in particular the clypeus and the mandibles, might relate to their feeding biology.

2. Materials and methods

The studied amber pieces came from the Hukawng Valley, near Tanai, Kachin state, in northern Myanmar, locality depicted in Dong et al. (2015, fig. 1). Burmese amber has been dated as originating in the early Cenomanian, at about 99–98 Ma (Shi et al. 2012). The pieces are deposited in the Department of Zoology (DZUP) of the Universidade Federal do Parana (UFPR) under care of the second author. In order to have a better view of the inclusions at least one surface of each piece was trimmed manually with a jewelry saw and/or ground with wet emery paper (grit sizes of 800–3000). The resulting pieces were hand polished using aluminum oxide (grits of 1 and 0.3 μm).

The fossils were studied using a Leica M125 stereomicroscope with 10× ocular lens. Lighting was provided by one or a combination of different methods: LED ringlight with adjustable lighting, spotlight illumination, and transmitted illumination through the base. Photographs were taken using a Leica DFC295 camera attached to the stereomicroscope. Images were improved using Zerene Stacker® software to combine multiple images then enhanced with Adobe Photoshop® (Adobe Systems). Some morphological structures are illustrated with line drawings using a camera lucida. Morphological terminology follows Keller (2011) for general morphology, Richter et al. (2019) for head morphology, Harris (1979) for sculpturing, and Wilson (1955) for pilosity. Since prognathy is a defining trait of ants (Bolton, 2003), a dorsal perspective of an ant head implies viewing the clypeus and frontal area, and sometimes a portion of the vertex (Richter et al., 2019), while a posterior perspective covers the occiput and part of the vertex. This convention, however, is strained by haidomyrmecines due to their clypeal expansion, which rotates part of the head almost 90° and leaves the dorsal cephalic view covering most of the clypeus, with the frontal area visible mostly in a posterior view. This difficulty is illustrated by fig. 1A, C in Perrichot et al. (2020), which depicts haidomyrmecine heads in two different perspectives, full-facial view and dorsal view respectively, but taxonomic descriptions of extant ants regard a full-facial view and dorsal view as the same perspective.

If these terms were to be consistent with the descriptions of extant ants, their full-face view would be dorsal and their dorsal view would be posterior. Additionally, the haidomyrmecine pre-oral cavity is directed ventrally as well as the mandibular base and the postgenal bridge in haidomyrmecines appears to be relatively shorter when compared with extant ants. This is relevant as a reduced hypostomal bridge is typical of most Hymenoptera (Beutel and Vilhelmsen, 2007), as well as orthognathy (hypognathy) (Burks and Heraty, 2015), implying that haidomyrmecines may not be as prognathous as crown ants, and offering another possible explanation for the difficulty in visualizing what is dorsal and posterior in the head capsule of these ants. For the sake of facilitating comparisons with previous haidomyrmecine descriptions, we adopt the conventions of Perrichot et al. (2020) regarding full-face view and dorsal view, as well as their putative prognathy. The full-face view faces the clypeus, whilst the opposing ventral view faces the postgenal bridge and postocciput; the dorsal view faces the frontal area and vertex, whilst the opposing anterior view faces the mandibular base and pre-oral cavity. The present convention, nevertheless, potentially obscures the comparison of homologous structures between these ants and extant ants. We urge the undertaking of more comparative studies between crown ants and stem ants that may illuminate some of the steps in ant evolution, particularly regarding the head.

The specimens were measured using an ocular micrometer calibrated for each change of magnification. Measurements used in the descriptions, including their abbreviations, are detailed in Table 1. Two different angles for measuring the head width are used here in an attempt to quantify the degree of vertical vs. horizontal elongation of the head capsule, hence projections, such as those of *Ceratomyrmex* Perrichot, Wang & Engel, are not included except when considering TL. General eye shape in these ants may be vertically elongate, horizontally elongate or somewhere in between, as such the traditionally defined OI (used here) captures but one relation between eye size and head size. Another relation is used in the descriptions when the eye length is related to the head length, in this case eye length is vertical, parallel to head height. Our definition of ML (mandibular length) differs from that (MDL) of Perrichot et al. (2020) by including the so-called "basal tooth" of most other authors of haidomyrmecines. We interpret this "basal tooth" as the main mandibular shaft, as proposed in Lattke et al. (2018), and regard their "tip of the mandible" as the apex of a preapical, dorsal mandibular tooth.

Exclusion of the "ventral tooth", a part of the mandible, implies that MDL measures just the length of the dorsal tooth. Some definitions of PH for extant ants consider the apex of the subpetiolar process but this is frequently hidden from view in fossils, so it is ignored here. If a feature does not lend itself to being measured it is scored as n/a. Most of the following measurements are graphically defined in Fig. 1.

3. Systematic paleontology

Formicidae Latreille, 1809
Sphecomyrminae Wilson and Brown, 1967
Haidomyrmecinae Bolton, 2003

Ceratomyrmex Perrichot et al., 2016

Emended worker diagnosis. Ocelli well-developed. Head with elongate projection arising dorso-anteriorly from between antennal insertions. Projection longer than half-length of scape; apex enlarged, either dorsoventrally flattened or club-like; ventral surface of apex studded with patches of apically truncate spicules, lateral apical margins and remainder of ventral face with numerous dangling long, hairs. Clypeus with median longitudinal carina. Mandibular dorsal tooth elongate and narrow, apex bluntly pointed almost reaching apex of cephalic projection. With mandibles closed, dorsal teeth diverge from each other close to apex. Two pairs of long trigger hairs stem from just anterad base of cephalic horn, midway between compound eyes.

Ceratomyrmex planus sp. nov. Lattke and Melo
(Figs. 2, 7A)

LSIDurn:lsid:zoobank.org:act: 6923F70D-4291-4AE3-B16C-F17919ED1E01

Diagnosis. Head between antennae projects anterodorsally as elongate, relatively straight horn, slightly surpassing one-half of scape length; apex swollen into modest club. Eye vertically elongate and facing dorsally; surface weakly convex, almost flat, barely above level of surrounding integument. Petiole sessile, node with vertical anterior face.

Description. Holotype worker. Measurements and indices. Hh 0.7; FrHW n/a; HL 0.5; SL 0.4; HoL 0.4; EL 0.2; ML 0.8; WL 1.1; MetL 0.9; PL 0.5; PH 0.3; TL 3.5 mm. FrCI n/a; LatCI 74; MI 130; SI 80; OI 40, HoI 100.

Table 1
Measurements, including abbreviations, used in the descriptions.

Abbreviation	Measurement	Explanation
Hh	Head height	Maximum vertical length of the head capsule, in either dorsal or lateral view, as measured from the anterior clypeal margin to the posteriormost point, excluding projections or horns.
FrHW	Frontal head width	Maximum horizontal head width, excluding the eyes, with the head in full-face or dorsal view. Considered as parallel to a line between the midpoint of the eyes.
HL	Head length	Maximum horizontal head length of the cephalic capsule from its anteriormost point to its posteriormost point, with the head in lateral view. Projections such as horns are excluded, in which case the measurement is taken from the base of the projection. A dorsal view may also be used.
SL	Scape length	Length of the first antennal article, excluding the neck and basal condyle.
HoL	Horn length	Straight line distance from base of elbow between vertical and horizontal ventral surfaces of horn to anteriormost point of horn with head in lateral view.
EL	Eye length	Maximum length of the compound eye.
ML	Mandibular length	Straightline distance from the apex of the dorsal tooth to the apex of the main mandibular shaft ("ventral tooth" of other authors) or basal angle.
WL	Weber's length	Diagonal length of mesosoma (or alitrunk) in profile, from anteriormost point of pronotum to posteriormost point of propodeum.
MetL	Metatibial length	Maximum straightline distance from the base of the metatibia to its apex, excluding setae and spurs.
PL	Petiolar length	The maximum straightline distance along the longitudinal axis of the petiole from its anterior margin to the posteriormost point of the tergite. Visible in lateral, dorsal or ventral view.
PH	Petiolar height	The maximum straightline vertical distance from the ventral margin at the petiolar midpoint to a horizontal line tangent to the dorsalmost point of the node. Measured in lateral view.
TL	Total length	Summed distance of HL + cephalic projection + WL + PL + gastral length, excluding the sting. It can be measured in lateral or dorsal view.
FrCI	Frontal cephalic index	FrHW/Hh × 100.
LatCI	Lateral cephalic index	LatHW/Hh × 100.
MI	Mandibular index	ML/Hh × 100.
SI	Scape index	SL/HL × 100.
OI	Ocular index	ED/HL × 100.
HoI	Horn index	HoL/SL × 100.

Head in lateral view with broadly convex posterior margin, convexity sharper at highest point just posterior to eye and close to ocellus, then gradually descending dorsad with brief convexity at base of clypeal projection. Only one ocellus discernible. Anterior clypeal margin weakly concave in lateral view, oblique, descending from base of cephalic projection, median clypeus elevated over lateral clypeal margins forming low, distinct longitudinal carina; dorsal base of clypeal horn in lateral view weakly convex. Hypostoma about as high as basal width of dorsal mandibular tooth, ventral surface convex. Posterior clypeal margin protrudes dorsoanteriorly as elongate, relatively straight horn, slenderer medially than at base or apex, apex swollen into modest club. Anterior face of projection with hanging flagellate hairs thicker at base, hairs longest on apical half, longest hairs 2× as long as apical horn width, basal half with fewer hairs, dorsal lateral margin of horn apex with curved semierect hairs, anterior apical face with apically truncate spicules. Long flagellate hairs hanging from clypeus between eyes and base of horn, including two pairs of trigger hairs.

Eye in lateral view elongate, vertical axis longer than longitudinal axis; eye facing dorsally, weakly convex, almost flattened, eye surface slightly elevated over surrounding integument. Torulus facing anterolaterally, in lateral view at mid-eye height, halfway between eye and base of horn. Radicle of scape arched, funicular segments subcylindrical, base of each slightly constricted, lateral margins of each weakly convex, last segment bluntly pointed. Scape weakly arched with sparse decumbent hairs, some thick. Pedicel as long as wide and half as long as flagellomere I, first flagellomere 3.4× longer than wide and similar in length to second flagellomere, flagellomeres II–X 3× longer than wide. Mandibles articulated within head, slightly separated from each other, internal faces weakly diverging at apex; mandibular base short and straight in lateral view; dorsal tooth slender, arching broadly and evenly, width mostly even from base to apical third, then gradually tapering to blunt point with two short setae, apex of tooth not quite reaching apex of horn; mandibular shaft projecting inward and ventrally as slender triangular tooth. Limited translucency of

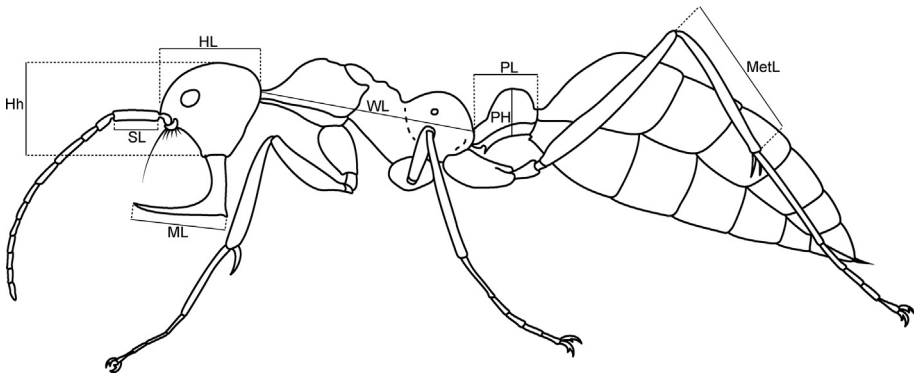

Fig. 1. Schematic lateral habitus of a worker haidomyrmicine ant, with indication of the measurements used in the description. See text for abbreviations. Figure modified from Dlussky (1996).

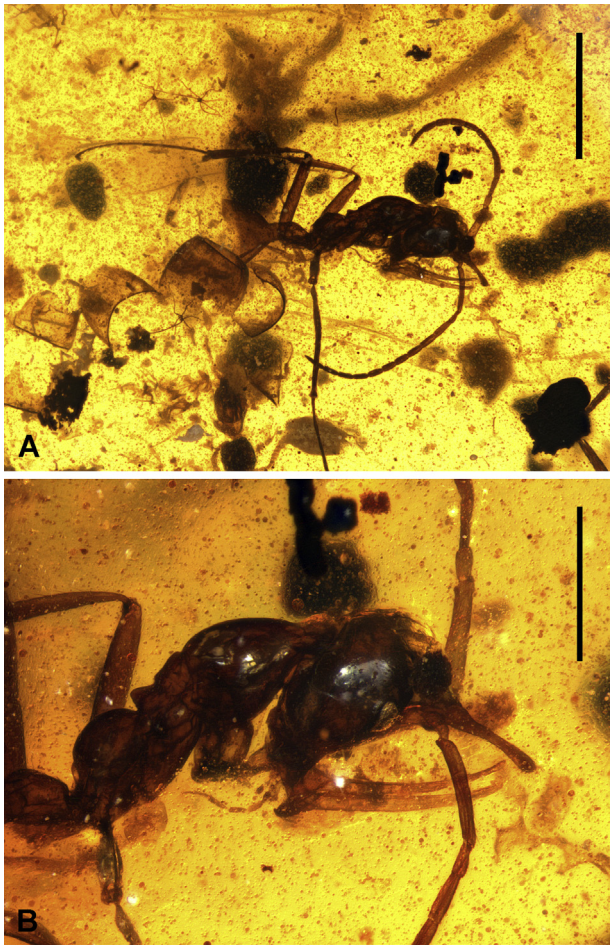

Fig. 2. †*Ceratomyrmex planus* Lattke and Melo, sp. nov., worker holotype, DZUP 548866 (Bur-557). (A) Habitus, lateral view; (B) Head and mesosoma, lateral view. Scale bars: A: 1 mm; B: 0.5 mm.

mandible suggests 5–6 long hairs or setae present on internal face of ventral "tooth". Palpal formula 5, 4. Maxillary palp with basal article thickest, palpomere II 2.5× longer than wide, palpomeres III and IV 2× longer than wide; apical palpomere longest, slenderer than rest. Palp with scattered erect hairs. Labial palp short, not extending beyond second maxillary palpomere, all sclerites slightly separated from each other, apical palpomere about twice as long as wide with bluntly pointed apex, preceding articles rounded. Three labial palpomeres clearly visible, basal article partially visible within buccal cavity.

Mesosoma in lateral view with convex pronotal dorsal margin, broadly convex anterad, more curved posterad, mesonotal dorsal margin straight and inclined, higher anterad than posterad, anterior margin higher than pronotum; mesometanotal sulcus well-impressed. Pronotum smooth, pronotal neck without lateral ridge. Propleuron broadly convex, higher posteriorly than anteriorly. Metanotum shaped as convex cone in lateral view, dorsal margin length three-fourths that of mesonotum. Lateral mesopleural area shaped as elongate convexity, smoothly curving to ventral face, lacking anteroventral carina. Murkiness of piece does not permit discernment of mesometapleural suture. Propodeal dorsal margin mostly convex with brief anterior shallow concavity, dorsum curves evenly to declivity. Propodeal spiracle placed at midlength and midheight of propodeum, opening slit-shaped and vertical, facing posterolaterally. Small dome-shaped elevation situated next to dorsal margin of mesopleural area and posterior to metanotum, possible metanotal spiracle.

Metapleural gland opening rounded, facing laterally, exposed. Propodeum and petiole with scattered erect – suberect hairs, longer than hairs of promesonotum. Petiole sessile, relatively low in lateral view, node with vertical anterior face, dorsally convex, weakly descending to posterior margin. Petiolar ventral margin in lateral view broadly convex, no anteroventral process discernible; tergosternal articulation visible as elongate, anteriorly converging triangle on posterior half of petiole, anterior half not discernible. Node dorsum with broad longitudinal rugosity and scattered erect to suberect, arched hairs. Procoxa and mesocoxa on one side each missing apical half, other foreleg only with coxa and part of femur visible. One disarticulated median leg located just anterad head with most of coxal base missing. Mesotrochantellus narrow and poorly-developed; mesotibia with one preapical seta and two apical spurs; mesobasitarsus with subdecumbent hairs and at least one median narrow seta close to midlength. Metatibial apex with one long pectinate spur and second shorter, simple spur, no pre-apical setae detected but posterior pre-apical edge with row of subdecumbent to decumbent, thick hairs that cover length of one-eighth tibial length, hairs not longer than half apical tibial width; metabasitarsus with abundant decumbent straight hairs, slightly longer than width of tarsus, apical half with at least two decumbent setae. Apex of tarsomeres with at least two setae; inner margin of pretarsal claws toothed, arolium developed.

Abdominal segment III anteriorly constricted into brief but distinct tubular neck, posterior margin of node fits into anterior AIII almost seamlessly, prora discernible as low transverse rounded crest. Abdominal tergite III much larger than sternite III, spiracle located anteroventrally on tergite, close to anterior constriction; anterior margin of tergite in lateral view arches evenly posteriorly. Dorsal margin of tergite III in lateral view slightly constricted posteriorly; posterior width lesser than at midlength, suggesting presence of shallow cinctus. Total disarticulation of the metasoma after abdominal segment III renders identity of associated but unattached sclerites uncertain. Fourth abdominal segment separated from body, tergite and sternite united, articulation not discernible; spiracle round, anterolaterally placed on tergite. Abdominal tergite and sternite V separated from each other. Pygidium laterally compressed, with abundant long hairs; sting aparatus missing.

Etymology. The species epithet is derived from the Latin adjective for flat, *planus*, in allusion to the flattened compound eyes of the worker of this species.

Type material. Holotype worker DZUP 548866 (Bur-557), in an oval amber piece measuring 19 mm long × 12 mm wide and maximum thickness of 5 mm. Piece with numerous inclusions, including abundant dirt, plant trichomes, one small parasitic wasp, one bethylid wasp, and a beetle. Partial remains of another, apparently conspecific, larger ant also present: mesosoma without prosternum and front legs, one middle leg present, and metacoxae. The holotype is complete except for missing most of the forelegs; one middle leg is disarticulated but positioned anterolaterally to the head; the gaster is mostly disarticulated but near the body; one posterior leg and both scapes are laterally compressed.

Discussion. *Ceratomyrmex planus* becomes the second species of *Ceratomyrmex* to be found, fitting well into the generic diagnosis of Perrichot et al. (2016), but with the following characters needing review to take into account this new species. The cephalic projection can not be considered just curved and apically spatulate as it is relatively straight and with an apical club in *C. planus*. Neither can the dorso-anterior development of the projection be considered as extending dorsad (above) the cephalic dorsal margin, as it fails to do so in *C. planus*. The trigger hairs do flank the dorsal mandibular teeth as described by Perrichot et al. (2016), but we feel it is more informative to state where they are issuing from on the head and have modified the generic diagnosis to reflect this. We have added

additional characters such as the presence of a median clypeal carina, the elongate and narrow shape of the dorsal mandibular teeth, their bluntly pointed apices, and the diverging apices of the mandibular dorsal teeth. The diagnostic usefulness of the presence of ocelli and a subpetiolar process for recognizing *Ceratomyrmex* is now rendered obsolete by *Dilobops* gen. nov., and *Haidomyrmex davidbowiei* sp. nov., as the former has ocelli and both have a subpetiolar tooth. Both the protibial and mesotibial apices in *C. ellenbergeri* were described as having three spurs but Fig. S1 in Perrichot et al. (2016) suggests that two of the protibial spurs could actually be preapical setae, and indeed these are redescribed as such (one spur and two setae) in Perrichot et al. (2020). The probasitarsus in *C. ellenbergeri* has a pecten formed by a row of short uniform hairs but the holotype of *C. planus* is missing most of the forelegs. This could be another generic character but better preserved specimens are needed for corroboration. The dangling hairs of the projection in the holotype of *C. ellenbergeri* include many flattened hairs, but these are simple in *C. planus*. *Ceratomyrmex planus* is a smaller ant than *C. ellenbergeri*, with a TL of only 3.5 mm compared with up to 5.9 mm for the holotype of *C. ellenbergeri*. For calculating TL we included the horn length. The horn length in *C. planus* is only 0.4 mm compared with 1.25 mm for the paratype of *C. ellenbergeri*. The node in *C. ellenbergeri* has a convex anterior margin in lateral view but in *C. planus* has a distinct vertical margin. The eye in *C. planus* is approximately twice the length of its width, though a full view of the eye is not possible without further trimming of the amber piece. If the key for identifying haidomyrmecine genera and species by Perrichot et al. (2020) is used for this species, it will key without problems to couplet 7, where it will mostly fit *Ceratomyrmex ellenbergi*, except for the shorter clypeal horn and dorsal mandibular tooth ("apical mandibular portion"). The characters used in the diagnosis for this species should suffice for separating between the two *Ceratomyrmex*.

Dilobops Lattke & Melo gen. nov.
Type species: *Dilobops bidentata* sp. nov.

LSIDurn:lsid:zoobank.org:act: 0C12695C-C731-44B3-8BD9-5448E32AC6CF

Diagnostic description. Three well-developed ocelli present, frontal area with short dorsomedian prong projecting dorso-anteriorly. Posterolateral clypeal margins with rounded projecting lobes in cephalic full-face view, lobes appearing as acutely pointed projections in dorsal or ventral view; dorsal clypeal surface without posteromedian elevation or longitudinal carina; distinct clypeal triangle not visible. Spiculae of setal patch acutely pointed. Long, flagellate (trigger) hair inserted close to anterolateral margin of setal patch. Length of pedicel over one-third that of scape. Probasitarsus with 1 seta and no row of setae or pecten.
Etymology. The genus is named in reference to the peculiar lobes projecting laterally to the clypeus, around the setal patch, from the Greek, *di-*, two, *lobos*, lobe and *ops*, face. The name is feminine.

Dilobops bidentata Lattke & Melo sp. nov.
(Figs. 3–5, 7C)

LSIDurn:lsid:zoobank.org:act: 4564CB71-0F32-45EA-97A5-75E717522EFB

Diagnosis. See genus description.
Description. Holotype worker. Measurements and indices. Hh 0.7; FrHW 0.6; HL 0.6; SL 0.3; EL 0.4; ML n/a; WL 1.6; MetL 1.2; PL 0.4; PH 0.2; TL 4.1 mm. FrCI 86; CI 86; SI 50, OI 50. Head elongate and widest posteriorly in anterior (full-face) view, dorsal margin (between eyes) convex, lateral cephalic margin (between eye and clypeus) broadly convex, lateral margins converging ventrally. Cephalic dorsal margin, from base of horn to vertex, in lateral view convex, descending sharply posteriorly to posterior ocelli; posterior margin broadly convex, slightly oblique; head barely discernible ventrad of eye level. Three round and distinct ocelli present, each weakly convex, anterior ocellus situated between eyes, distance between anterior ocellus and posterior ocelli greater than that between posterior ocelli, posterior ocellus situated posteriorly to eye. Vertex smooth and shining. Eye situated laterally on head close to lateral cephalic mid-width and occupying almost one-third of

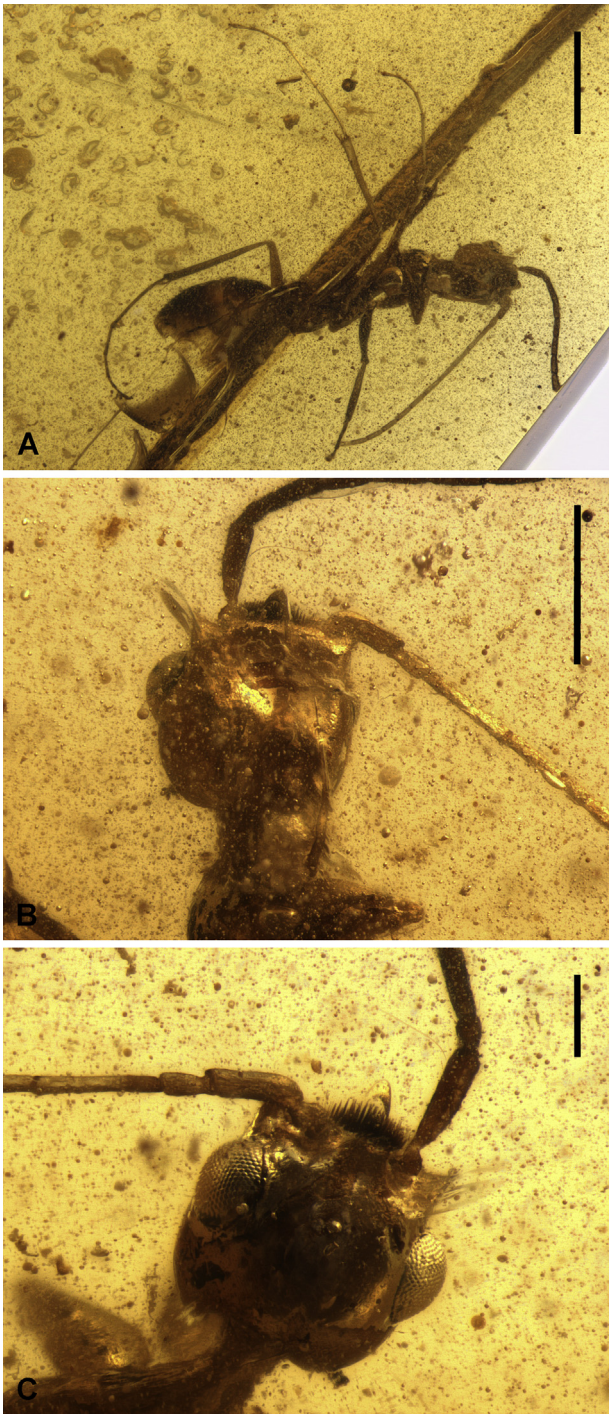

Fig. 3. †*Dilobops bidentata* Lattke and Melo, gen. et sp. nov., worker holotype, DZUP 548867 (Bur-033). (A) Habitus, ventral view; (B) Head, ventral view; (C) Head, dorsal view. Scale bars: A: 1 mm; B: 0.5 mm. C: 0.2 mm.

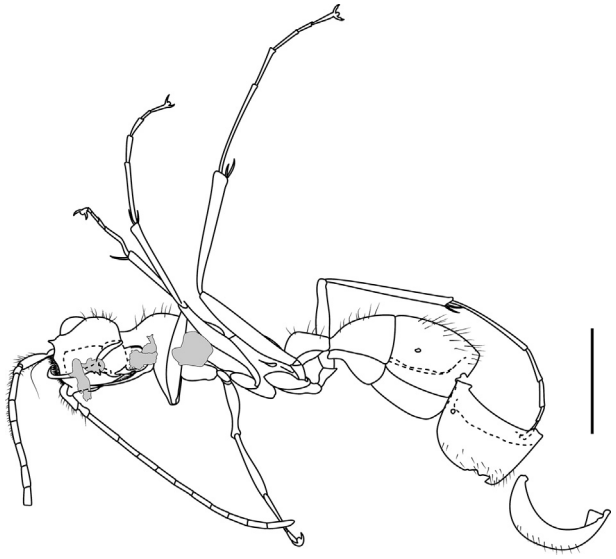

Fig. 4. †*Dilobops bidentata* Lattke and Melo, gen. et sp. nov., illustration of holotype body, ventral view. Scale bar: 1 mm.

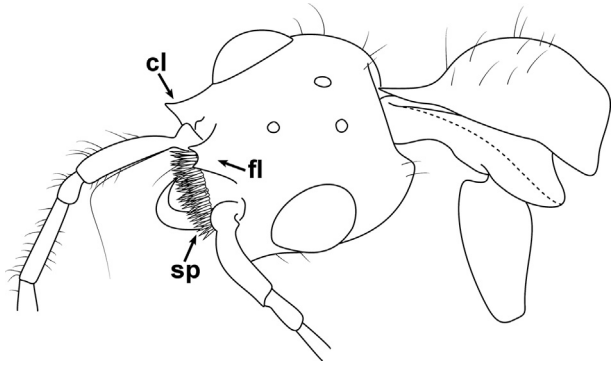

Fig. 5. †*Dilobops bidentata* Lattke and Melo, gen. et sp. nov., illustration of holotype head, dorsal view. cl – clypeal lobe, fl – frontal lobe, sp – setal patch.

lateral cephalic margin. Eye convex in cephalic anterior view, in cephalic lateral view oval, ommatidia abundant, no pilosity discernible on eye. frontal area posterior to antennal insertion with median dorsal lobe, base not wider than distance between antennal sclerites. Frontal lobe ends with two stout but pointed teeth; lobe slightly overhangs posterior margin of setal patch in lateral view, not higher than two scape widths.

Antennal sclerite placed on shelf-like projection between setal patch and dorsally to lateral clypeal lobe, insertion anterolaterally directed; torulus forms low rim, frontal carina absent. Antenna 12-merous, flagellum filiform, with apical flagellomere ending in blunt point, one antenna missing flagellomeres VII–X. Antennal scape 4–5 times longer than wide, shaft mostly straight, sides subparallel, basal arch begins with minor constriction, then expands into lobe not wider than scape width before basal constriction, bulbus exposed; scape bent at base. Pedicel stout, slightly constricted at base, length 0.38 of scape; flagellomere I four times longer than width and longer than flagellomere II, funicular articles cylindrical and elongate. Scape, pedicel, and flagellomere I with sparse, erect to suberect hairs, longest hair about as long as maximum scape width. Hairs with length proportional to respective segment width, with density of hairs thinning apicad.

Most of clypeus shaped as longitudinally elongate concavity with length close to sixty percent of head in anterior view, slightly wider dorsad than ventrad; ventral clypeal margin convex, bordered by carina. Dorsal clypeus overhangs concavity, includes setal patch and lateral lobes. Setal patch shaped as transverse elongate-ovoid, dorsal margin not surpassing antennal insertions, width less than two scape widths; patch with 50–60 abundant stout and straight spiculae, each with pointed apex; brown color, darker than surrounding integument. Dorsolateral clypeal lobe subquadrate with rounded vertices, dorsal margin longer than anterior margin, projecting latero-anteriorly to form a pointed corner in dorsal or ventral views. Abundant fine, erect hairs present ventrally to setal patch. Long, flagellate (trigger) hair inserted close to ventrolateral margin of setal patch, hair length close to length of dorsal mandibular tooth, exact point of insertion not clearly discernible; other trigger hair separated from head. Other long and fine hairs also present, apparently coming from setal patch, about one fourth length of "trigger" hair. Mandibles very diaphanous. Best conserved mandible with dorsal tooth positioned vertically, tooth straight to weakly arched at basal two-thirds, then curving more towards head, apex touching setal patch ventrolaterally, base of mandible not visible. Tooth smooth. Other mandible separated from head at anterolateral position, base not visible. Pronotum with convex anterodorsal margin in lateral view, mesonotum forming modest convexity, promesonotal articulation forms shallow depression. Pronotal neck elongate; propleura partially separated from pronotum, ventral surface relatively flat. Posterolateral pronotal margin forms blunt obtuse angle. Lateral mesopleural area without carina separating it from ventral face, rounding onto ventral face. Propodeal dorsum margin in lateral view forming strong convexity, depression between mesonotum and propodeum shallow, propodeal dorsal margin mostly straight, propodeal declivitous margin convex. Trochantellus present. Protibial apex with pectinate spur that reaches one-fourth of basitarsal length, protarsal basal arch with single seta, no row of setae nor pecten. Mesotibial apex with two spurs. Metatibial apex with two spurs and at least one seta, one spur partially pectinate with comb developed on apical half, accompanying spur simple and at least two-thirds as long as pectinate spur. Metatarsomeres elongate, each apex with 4 slender setae, tarsomeres 1–3 parallel-sided, 4–5 wider apicad than basad; metatarsal claws slender, toothed, length approximately one-third that of apical metatarsus, rounded aroleum present. Basal metatarsus about as long as articles 2–5 combined. Metacoxa longer than mesocoxa.

Node relatively low and convex in lateral view, highest anterad, anterior margin convex, dorsal margin twice as long as anterior margin. Line between petiolar tergite and sternite distinct, sternite in lateral view with ventro-anteriorly expanding lobe, anterior margin not visible due to leg on one side and long antenna on other side. Posterior petiolar margin covers abdominal pretergite III. Abdominal tergite III in lateral view with anterior margin broadly convex, gradually ascending posterad from petiole. Sternite III broadly convex in lateral view, not fused with tergite III as some separation apparent between them. Prora not discernible. Cinctus weakly developed but distinct, posterior margin of postergite III forms brief drop, anterior margin of postergite IV with brief shallow constriction. Tergite III with scattered suberect hairs, posteriorly directed, longest hairs not longer than half length of metatarsus II. Abdominal tergite IV and sternite IV separated from gaster and from each other, posterior margin of each tattered. No pubescence discernible. Body mostly smooth with scant sculpturing.

Etymology. Named in reference to the double pointed prong on the frontal area, from the Latin *bi-*, two, and *dentata*, provided with teeth.

Type material. Holotype worker DZUP 548867 (Bur-033). The amber piece is mostly rounded, measuring 16 mm × 18 mm with two straight margins. The thickness of the piece ranges from 5 to 3 mm. Two thirds of the piece has numerous small bubbles, except for spot with fossil, which is close to the intersection of the two linear margins. Visibility of anterior cephalic regions is difficult to nil. Lateral view of mesosoma partially blocked by ant's own legs and large antennae of other insect inclusion. The specimen's body is more or less straight. Because of the way the amber was polished it is possible to only clearly see slightly more than one half of the head dorsally. Part of the head is more distorted, with the curvature of the eye appearing exaggerated, globulose, and its position seems to be more posteriorly placed. The complete antenna is clearly more elongate and diaphanized than the other and is thus considered deformed, so the relative lengths and widths of the antennal segments are gleaned from the incomplete, but dark, antenna. The head width could not be accurately taken in a anterior view so it was taken in a dorsal view, a perspective offering much clearer view and with apparently little distortion and in a position favorable for gauging its width. Hh is a rough estimate as it was taken in an oblique lateral view of the head and the anterior head region is not visible. WL and TL were taken in a lateral view of the specimen but the longitudinal axis of the specimen is somewhat oblique to the amber surface such that the actual values should be a bit more than those registered.

Discussion. This ant is quite distinct amongst the haidomyrmecines on account of the bidentate frontal lobe. In other haidomyrmecines, the frontal triangle is either pyramid shaped in genera lacking a clypeal horn, or if a horn is present, it is indistinct and apparently fused with the base of the horn (Perrichot et al., in review; Barden et al., in review). When distinct, the haidomyrmecine frontal lobe is adjacent to the clypeal setal patch, but in *Dilobops* gen. nov. it is distinctly separated from it and posterior to the antennal sockets. *Protoceratomyrmex revelatus* Perrichot et al. (2020) has a raised rectangular process between antennal sockets that may represent the frontal triangle, but the more posterior positon of the lobe in *Dilobops* suggests these structures may not be homologous. The posterolateral clypeal lobes are another trait lacking in known haidomyrmecines. Some of the spicules of the setal patch seem to be of a composite nature with an internal dark seta surrounded by a lighter-colored sheath. The clypeal trigger hairs in *Dilobops* are difficult to discern, particularly their points of insertion in the head. Examination of the specimen suggests the presence of two pairs of hairs, one pair issuing from the setal patch and another from a site anterolaterad of the patch. These ants vary considerably in the location and in the paired-unpaired condition of the trigger-hairs. In *Haidomyrmex* Dlussky, *Haidomyrmodes* Perrichot et al., and *Haidoterminus* MacKellar, Glasier & Engel there are two sets of paired hairs and they stem from various positions within and about the setal patch (Perrichot et al. 2016, V. Perrichot pers. com.). In *Ceratomyrmex* there are two adjacent pairs between the eyes at the base of the clypeal horn (Perrichot et al. 2016). *Protoceratomyrmex* Perrichot et al. has a pair of hairs on the posteromedian clypeus, next to the clypeal horn. In *Linguamyrmex* Barden & Grimaldi single pair of trigger hairs stem from the middle of the setal patch on the clypeal projection (Barden et al. 2017). In *Haidomyrmex davidbowiei* sp. nov. two hairs dangle from the dorsal anterior surface of the clypeal shelf, posterior to the setal patch. It is possible that due to artefacts (abrasion, taphonomic processes) the paired-unpaired nature of the hairs in some of these taxa may be erroneously interpreted.

The subpetiolar process of *Dilobops* is lobe-like, but in other haidomyrmecines it may be absent or toothed. Ocelli are either absent or atrophied in *Haidomyrnex*, but this species has very distinct ocelli. The clypeus in *Haidomyrmex* and *Haidoterminus* have a median elevation that may be either mostly posterior or mostly anterior, but the whole clypeus in *Dilobops* is shaped as a broad sulcus, without a median raised area. These differences in clypeal shape may affect the area for attachment of the muscles controlling the cibarium and imply differences in feeding biology. The relative length of antennal pedicel is unique in this ant due to its length, over one-third of the scape length. In all other haidomyrmecine ants the pedicel is short, under one-fourth the scape length. The length of flagellomere II is 75% that of flagellomere I in one antenna and 68% in the other. If the key to haidomyrmecinae genera and species by Perrichot et al. (2020) is used with this species it becomes difficult to move beyond the second couplet as even though it agrees with the antennae being elongate, it also disagrees because the first flagellomere is longer than the second flagellomere.

Haidomyrmex davidbowiei Lattke & Melo, sp. nov.
(Figs. 6, 7B)

LSIDurn:lsid:zoobank.org:act: 95FE4267-CEFC-4E17-BF87-7B2E41587D95

Diagnosis. Two long, flagellate, trigger hairs issuing dorsomedially to setal patch. Flagellomere I longer than each of flagellomeres II–IX. Clypeus with ventromedian longitudinal convexity elevated above surrounding integument, gradually receding dorsad and becoming level with surrounding integument. Maxillary palp long, reaching close to one-fourth of mandibular length, labial palp short, not reaching apex of basal maxillary palpomere. Pecten of probasitarsus with fine hairs of uniform length and stout median seta. Mesotibial apex with no spur. Petiole sessile, dorsal margin of node in lateral view mostly convex with posterior shelf; petiolar ventral process toothlike.

Description. Holotype worker. Measurements and indices. HL 0.7; DorHW n/a; LatHW 0.7; SL 0.4; EL 0.3; ML 0.7; WL 1.6; MetL 1.0; PL 0.5; PH 0.3; TL 4.4 mm. DorCI n/a; LatCI 100; SI 57, OI 43.

Head in lateral view roughly as high as long, shaped as upside down triangle with convex dorsal base and briefly truncate ventral apex, dorsal cephalic margin extends from vertex to apex of frontal triangle, anterior cephalic margin concave, descending ventroposteriorly from frontal triangle to ventral clypeal margin. Posterior cephalic margin in lateral view forms brief, almost vertical margin from level of cephalic insertion with pronotum to same level as ventral margin of eye, most of dorsal head margin weakly convex and ascending anteriorly until at same level with posterior margin of eye, then descends along weakly convex margin to clypeal prominence, forming blunt obtuse angle with anterior clypeal margin. Clypeus protrudes anterodorsally between antennal insertions as brief convex lobe that forms shelf overhanging ventral clypeal margin, ventral face of lobe with oval setal patch, with long pointed setae on anterior half and peg-like spiculae on posterior half, two trigger hairs protrude anteromedially of patch. Ocelli absent. Eye semispherical in dorsal view, broadly elliptical in lateral cephalic view, placed anterodorsally on head close to antennal insertion. Antennal insertion between eye and clypeal setal patch, dorsolaterally projecting; scape at least 3.8× longer than maximum width, mostly straight, gradually widening apically, base not visible due to fissure in amber. Pedicel length less than one-fourth that of scape. Flagellomere I longer than each of flagellomeres II–IX but as long as X. Flagellomeres II–V each slightly longer than any of flagellomeres IV–IX; flagellomeres all of same width. Flagellomere I with subparallel sides, following flagellomeres with convex lateral margins and base of each flagellomere narrower than apex of preceding sclerite. Apical flagellomere sharply pointed with single long hair at apex. Leading edge of scape toward apex with row of at least 7–10 elongate-lanceolate shaped, decumbent to

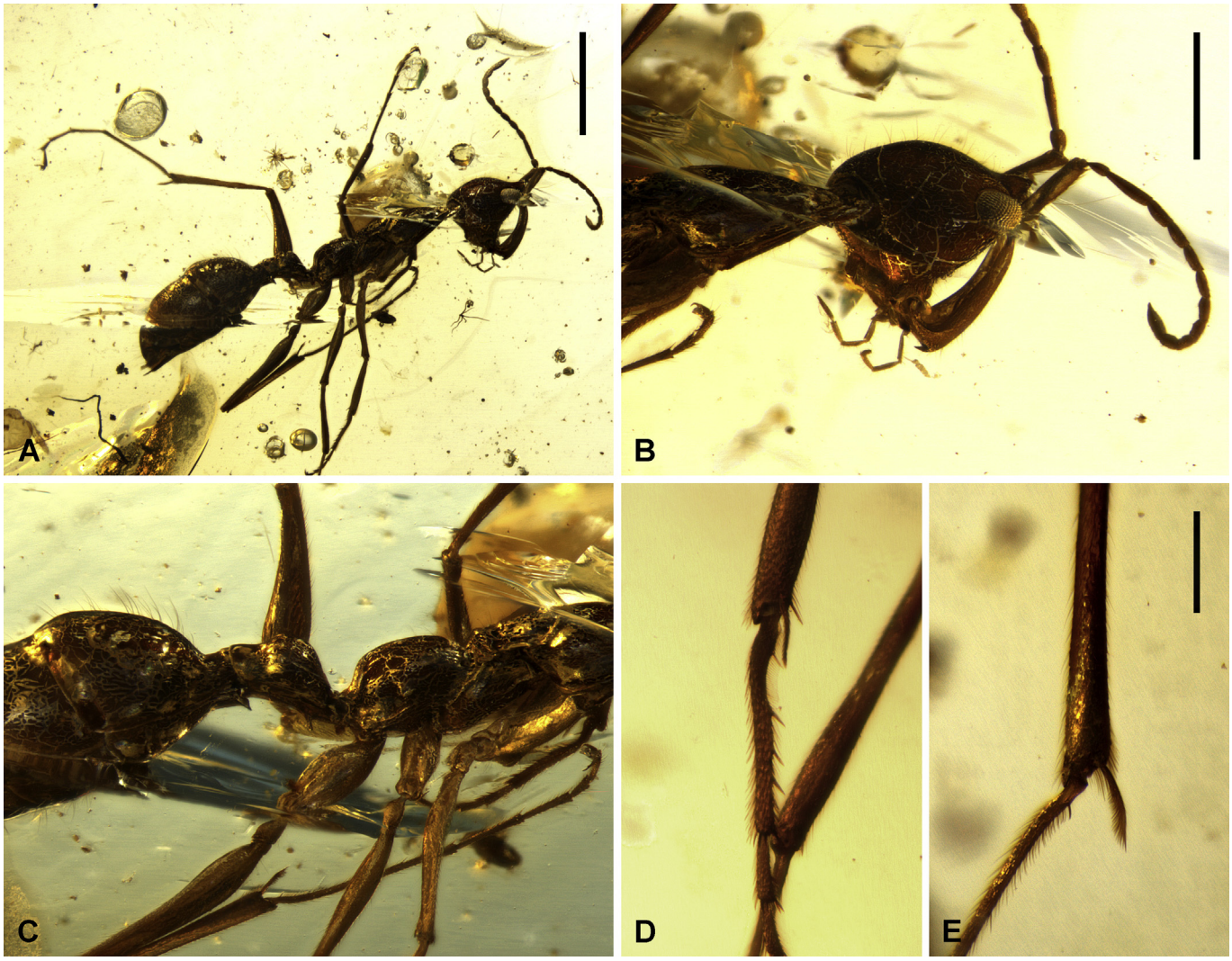

Fig. 6. † *Haidomyrmex davidbowiei* Lattke and Melo, sp. nov., worker holotype, DZUP 548868 (Bur-539). (A) Habitus, lateral view; (B) Head, lateral view; (C) Mesosoma and anterior portion of gaster, lateral view; (D) Detail of protibial apex and associated tarsi, inner view; (E) Detail of metatibial apex and its basal tarsus, inner view. Scale bars: A: 1 mm; B–C: 0.5 mm. D–E: 0.2 mm.

subdecumbent hairs, apparently flattened. Scape and funiculus with decumbent hairs, none longer than half width of their respective antennal sclerite, except for some lanceolate hairs on scape.

Anterior tentorial pit situated close to buccal cavity, forming base of vertical sulcus that fades away one-third distance between setal patch and anterior clypeal margin. Median clypeal area forms longitudinal raised rib of width about one-third of cephalic width, rib in lateral view highest anterad, gradually losing height dorsally, overhung by setal patch. Setal patch with elongate, acicular spicules, some longer than apical scape width, some apparently of composite nature with central dark seta or bristle surrounded by lighter-colored sheath. Anterior clypeal surface with scattered, ventrally inclined decumbent hairs. Head dorsolateral to clypeus with erect to suberect hairs, density increasing close to setal patch. Dorsal face of head with scattered erect to suberect hairs of varying lengths, longest hairs slightly longer than maximum scape width. Posterior cephalic surface with few hairs, mostly with scattered erect pubescence. Labrum projects anteriorly to form shelf not longer than half-length of mandibular basal arm, lateral margin convex, discal area with longitudinal low ridge. Lateral mandibular base with brief longitudinal ridge, mandibular shaft in lateral view arches anteroventrally; mandibular apex in anterior view appears as pointed triangular tooth with apex directed ventrolaterally, darker than rest of mandible and length more than half width of mandibular base in lateral view, apparently overlapping other mandibular apex, mandibles appearing asymmetrical. Dorsal tooth smooth, base placed ventral to eye level, tooth weakly and evenly arching in lateral view, relatively wide with series of discrete denticles on internal edge close to apex, apex touching ventral margin of setal patch. Mandibular dorsal teeth in anterior view with apices briefly diverging, tips separated by distance equal to pedicel width; dorsal edge of tooth with scattered erect to suberect hairs.

Maxillary palp relatively long, extending to one fourth of mandible length; pentamerous, articles II-V at least 4× longer than wide, each palpomere gradually widening apicad, palpomeres 1–4 apically truncate, palpomere V tapering apicad with 2–3 apical hairs. Palpomeres with scattered erect hairs, each as long as maximum width of each article or slightly longer. Only apical article of one labial palp totally visible, ante-apical article partially visible, recessed in buccal cavity; apical article oval in lateral view with

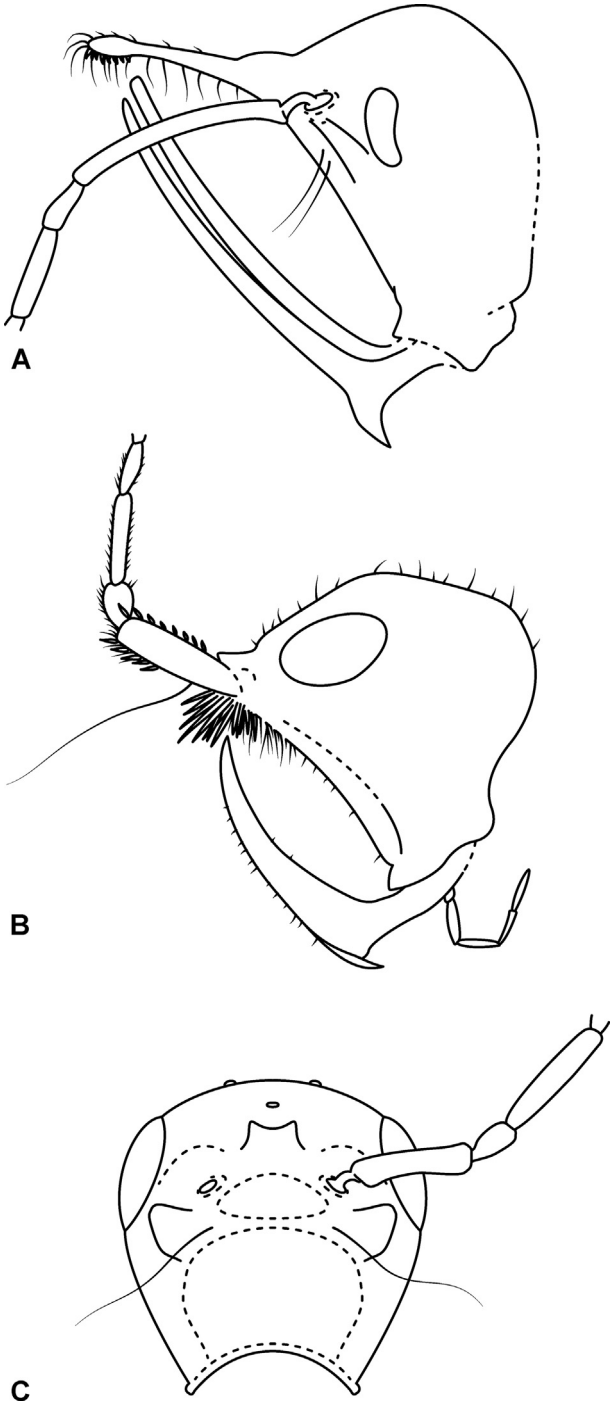

Fig. 7. (A) †*Ceratomyrmex planus* Lattke and Melo, sp. nov., illustration of holotype head, lateral view; (B) † *Haidomyrmex davidbowiei* Lattke and Melo, sp. nov., illustration of holotype head, lateral view; (C) †*Dilobops bidentata* Lattke and Melo, gen. nov. et sp. nov., schematic representation of head, frontal view. Not drawn to scale.

tapering apex, more than half as wide as long, robust, not elongate. Labial palp with scattered standing erect hairs, as long as palpomere width or shorter. Buccal cavity laterally bound by vertical ridge about as high as three-fourths length of apical maxillary palpomere, but medially about as high as palpomere; hypostoma ventrally bulging, anterior edge medially bilobed, lateral hypostomal lobe as high as ventral mandibular articulation. Occipital depression abrupt, not carinate, transverse and elongate-oval.

Mesosoma elongate in lateral view, dorsal pronotal margin broadly convex, laterally with low ridge that separates anterior pronotal face from pronotal neck, pronotal neck anteriorly projects as short flat rounded lobe in dorsal view. Posterolateral pronotal lobe slightly rounded, elevated, extending posteriorly to mid-length of mesonotum. Anterior mesonotal margin raised above posterior pronotal margin in dorsal view, mesonotal dorsal margin in lateral view weakly convex; mesonotum longer than wide in dorsal view. Propleuron relatively flattened, weakly convex; median sulcus between propleura visible, slightly depressed; prosternum visible as short triangle with bifid posterior apex. Metanotum in dorsal view wider than long, anterior margin concave; dorsal margin in lateral view convex, more curved than mesonotum. Metanotal-propodeal suture deep; bulbous structure next to dorsal mesopleural margin at metanotal – propodeal suture suggests metanotal spiracle but fissure impedes observation of details.

Mesopleural area dorso-anteriorly bound by ridge that anteriorly forms lobe with width one-fourth of lateral mesopleural width, lobe overhangs anteroventral margin; mesopleural area higher along mesometapleural suture. Mesometapleural suture well-impressed, oblique; posteriorly directed carina projects from mesometapleural suture becoming inconspicuous posteriorly but forming continuous elevation that joins with ridge that separates propodeum from metapleuron, defining lateral propodeal sulcus that arches posteroventrad, ventral margin of sulcus with ridge that begins anteriorly at spiracle. Metapleuron wider anterad than posterad, surface relatively flat, bound anteroventrally by low, broad convex ridge; dorsal and ventral ridges converge to metapleural gland orifice; no bulla evident; orifice facing posterolaterally or posteriorly. Propodeal dorsal margin in lateral view weakly convex, rounding smoothly to declivitous margin, declivity half as long as dorsal margin, declivity steeply dropping; propodeal spiracle place at mid-length and above mid-height of segment; orifice slit-shaped, vertical, slightly arched, facing posteriorly.

Trochantellus present, tarsal claws with pre-apical tooth closer to claw apex than base, arolium large. Protibial apex with large preapical seta and apical pectinate spur, spur with brief preapical lobe; pecten of probasitarsus with fine hairs of uniform length and stout median seta, 5–6 other stout setae present apicad to pecten; protibial setae stouter than setae of meso- and metatibiae; posterior protibial surface with abundant hairs. Mesotibia without discernible spurs, but with setae close to apex, mesobasitarsus with slender seta but no distinct basal seta. Visibility difficult because of position of both mesotarsi. Metatibia with posterior pre-apical edge bearing row of subdecumbent to decumbent, thick hairs that cover length of one-eighth tibial length, hairs not longer than half apical tibial width; metatibial apex with single pectinate spur and smaller simple spur one-third its length and no accompanying pre-apical seta. Metabasitarsus with stout slightly arched seta close to base, plus eight scattered straight setae, mostly concentrated on apical half; apex with two setae, stouter than other metatibial setae. Femora and tibiae with sparse decumbent pubescence throughout, and numerous suberect and subdecumbent hairs on dorsal edge of each.

Petiole sessile, dorsal margin of node in lateral view mostly convex with posterior shelf, anterodorsal margin longer than posterodorsal; posterior shelf weakly convex, about one-fourth length of petiole. Petiolar tergum bordered anterolaterally by carina that arches dorsoposteriorly to spiracular prominence, spiracle located at anterior one-third of petiole, close to ventral margin of tergum. Petiolar tergosternal line evident. Laterotergite distinct, shaped as elongate triangle, gradually widening posterad. Subpetiolar process anteroventrally directed as slender, parallel-sided lobe with blunt tip. Helcium axially placed, abdominal tergum III

and sternum III with anterior constriction with longitudinal costae, prora shaped as well-developed anteroventrally projecting lip. Pretergite III apparently normally covered by posterior tube-like extension of petiolar tergite but in specimen exposed on one side with dark ridge on anterior margin. Abdominal tergite II weakly longitudinally elevated ventrolaterally, forming overhang with ventral margin. Abdominal tergum III in lateral view with convex ascending margin, dorsal gaster highest at posterior margin of tergum III, dorsal margin of tergum IV mostly straight to weakly convex, posteriorly descending towards pygydium; gastral sternal margin in lateral view broadly convex; weak but distinct constriction present between pre and postsclerites of abdominal segments IV. Pygidium strongly arched, cross-section shaped as inverted "V". Spiracle of abdominal tergum IV round, relatively small, placed anterolaterally where lateral surface curves on dorsal surface. Spiracles of abdominal segment III not discernible, those of segments V-VII not visible. Gaster lacking pubescence, with scattered erect and suberect hairs, no setae on posterior margins of pygydium nor hypopygidium. Sting well-developed. Most of gaster smooth, lacking significant sculpturing.

Etymology. The species epithet is a patronym in honor of the artist David Robert Jones (1947–2016), known professionally as *David Bowie*.

Type material. Holotype worker DZUP 548868 (Bur-539) is included in a very clear piece with scant debris and shaped as half a heart. The piece measures 20 mm in length, maximum width of 10 mm and maximum thickness of 3 mm. A bethylid wasp, whose head has been sanded off, is also in the piece. Three more or less parallel fissures present affecting the specimen: one longitudinal across head at eye level and extending posteriorly to pronotum, one cutting across the head, anterior to eye margin and extending anteriorly; another cutting the gaster obliquely. A full-face view of head not possible, but lateral views and oblique lateral view of one side of head possible.

Discussion. This species agrees with most of the characters used by Perrichot et al. (2016) and Cao et al. (2020) to diagnose the genus *Haidomyrmex* except for the following: mesotibial apical spurs 0, absence of a long stiff seta on flagellomere I, flagellomere I longer than either flagellomeres II or III, point of origin of clypeal trigger hairs, only one pair of trigger hairs, and sessile petiole. The apparent lack or extreme reduction of the mesotibial spurs in this specimen is unusual as the usual tibial spur formula in Haidomyrmecinae is 1,2,2 (Perrichot et al., 2020), though *Haidoterminus* bears one metatibial spur (McKellar eet al., 2013). One mesotibia in this specimen offers a clear lateral view while the other offers a ventral, almost apical view of its apex. The first flagellomere is shorter than the second flagellomere in other *Haidomyrmex*, while in *H. davidbowiei* it is distinctly longer. The position of the trigger hairs in *H. davidbowiei*, posterior to the setal patch, is not shared with other species of the genus as well as their single-pair nature, the trigger hairs being double-paired in other *Haidomyrmex*. The stout median seta of the probasitarsal pecten is a trait that does not seem to be present in other *Haidomyrmex*. The descriptions and illustrations of *H. scimitarus* Barden & Grimaldi and *H. zigrasi* Barden & Grimaldi do not mention nor depict such a character. Neither is it mentioned in the redescription of *H. cerberus* by Cao et al. (2020), an absence further reinforced by their image (Fig. 1D) of a protibial apex and protarsal base. The petiole is weakly pedunculate in other *Haidomyrmex* and this species appears to have lost any anterior elongation of the petiole. The anteromedian clypeal elevation of *H. davidbowiei* is contrasts with the posteromedian elevation known for *H. scimitarus* Barden & Grimaldi and *H. zigrasi* Barden & Grimaldi, but in *H. cerberus* the elevation appears to be relatively uniform along its median length, without a noticeably anterior or posterior swelling (Cao et al., 2020). *Haidomyrmex davidbowiei* also has some sculpturing not described for other *Haidomyrmex*, such as the broad sulcus that borders the propodeum posterolaterally. The pennant-like hairs on the scape of this species are not known in other congeneric species. There seems to be some short stiff hairs between the ommatidia, each no longer than the diameter of each ommatidium, but they could be a taphonomic artefact.

4. Key to the species of Haidomyrmex

1. Flagellomere I longer than flagellomere II; two trigger hairs project from close to apex of clypeal lobe, posterior to setal patch; leading edge of scape toward apex with 6 or more elongate lanceolate hairs …. *Haidomymex davidbowiei* sp. nov.
   - Flagellomere I shorter than flagellomere II; two pairs of trigger hairs each project from within the setal patch; apex of scape with simple hairs …..…..… 2
2. Basal portion of mandible longer than half-length of dorsal tooth, mandible L-shaped in lateral view with dorsal tooth forming right angle with base; body with abundant pilosity, basal antennomeres and outer mandibular surface with dense pubscence ……..……..… *Haidomyrmex cerberus* Dlussky, 1996.
   - Basal portion of mandible under one-third of dorsal tooth length, mandible in lateral view with dorsal tooth forming acute angle with base; body with scattered pilosity, basal antennomeres and outer mandibular surface without pubscence …….....…….…..…..…..……. 3
3. Eye diameter in lateral view not more than one-fourth of head length, maxillary palps at least twice as long as ventral cephalic width; vertex without pilosity; basal portion of mandible relatively long, ventral corner with multiple asymmetrical teeth between mandibles; subpetiolar process absent ……....….... *Haidomyrmex scimitarus* Barden and Grimaldi, 2012.
   – Eye diameter close to one-third of head length; maxillary palps short, length not more than half the ventral cephalic width; vertex with few erect setae; basal portion of mandible relatively short, ventral corner a single asymmetrical tooth between mandibles; subpetiolar process shaped as minute tooth …….. *Haidomyrmex zigrasi* Barden and Grimaldi, 2012.

5. Haidomyrmecine morphology and natural history

The mandibular morphology of haidomyrmecine ants, and the peculiar cephalic projections of some species, has provoked much speculation regarding their structure, function, and the implications for their natural history. The L-shaped mandible in genera such as *Haidomyrmex*, *Ceratomyrmex* or *Linguamyrmex* is most frequently interpreted as having an upturned shaft, with a ventral-dorsal plane of movement for specialized predation (Barden and Grimaldi, 2012; Perrichot et al., 2016; Barden et al., 2017, Cao et al., 2020). Lattke et al. (2018) proposed that the haidomyrmicine mandible is mostly a hypertrophied, dorsally directed tooth based upon parallels in the mandibular morphology of extant ants such as *Protalaridris* Brown and *Harpegnathos* Jerdon. They also argued against a vertical plane of mandibular movement based upon the dorsal and posterior mandibular articulation of Dicondylia, that restricts movement to a lateral plane.

Even though the general haidomyrmecine cephalic shape is presently nonexistent amongst ants, it has contemporaneous analogs in several groups of scelionid, diapriid, and figitid parasitoid wasps. Some of these wasps, such as scelionids of the genus *Tyrannoscelio* Arias-Penna, Johnson & Masner, even have elongate, arched mandibles reminiscent of the state in haidomyrmecine ants

(Masner et al., 2007). Remarkably the plane of movement in these wasps is mostly vertical with some transverse arching, as documented in images and explained by Masner et al. (2007). The dorsal mandibular articulation is deeply invaginated and the ventral articulation is placed anterolaterally on the head. Other wasps with a similarly shaped head capsule and varying degrees of dorsoventral mandibular movement are figitid wasps of the genus *Stentorceps* Nielson & Buffington and *Nanocthulhu* Buffington (Nielson and Buffington, 2011; Buffington, 2012). A similar head shape is also present in a number of other parasitoids (Table 1 in Nielsen and Buffington, 2011), but mandibular movement is clearly lateral in almost all. These wasps differ from haidomyrmecines in having robust mandibles and an evident bulge or condyle at the dorsomedian mandibular base. If a cross-section at midlength of a *Tyrannoscelio* mandible is compared with that of a haidomyrmecine dorsal tooth, the wasp mandible is relatively quite thick and robust in contrast with the ant tooth. Examination of the present haidomyrmecine specimens, particularly that of *H. davidbowiei*, show a prominent ventral mandibular articulation, but not the bulge of the anterior articulation, corresponding to the dorsal – posterior joints of crown ants. Ongoing research by Keller et al. (2019) suggest a greater degree of mandibular movement in ants than in most other dicondylic insects. Given this morphological uncertainty, the results of new research (V. Perrichot, pers. comm.), and the above examples of vertical mandibular movement in other Hymenoptera, the case for vertical mandibular movement in haidomyrmecines is quite convincing. Hopefully careful analysis of the fossils may reveal the underlying morphological mechanism.

Were haidomyrmecine ants all predators, as seems to be the consensus? One specimen of *Linguamyrmex* even has an insect larva just within the reach of its mandibles, suggesting predation (Barden et al., 2017) and at least one fossil has a prey item caught between the dorsal teeth and the head (V. Perrichot, pers. com.). The dorsal tooth has a shallow longitudinal sulcus along the internal face that suggests facilitation of the flow of liquid. This has been noticed by several authors (Barden et al., 2017) and invoked as an adaptation toward hemolymph feeding in the context of the trap-jaw hypothesis, implying impalement of prey. Characters supporting a trap-jaw mechanism include the existence of so-called trigger hairs in these ants plus the apparent bioaccumulation of metals in the cephalic horn of *Linguamyrmex vladi* as detected by Barden et al. (2017). Trigger hairs are present in different lineages of extant trap-jaw ants and the presence of metal could aid in structural reinforcement due to the force exerted by mandibular impact. The dorsal tooth and head of *Dhagnathos autokrator* Perrichot et al. have a series of denticles that form an effective trap for prey. Such evidence reasonably supports prey securement with the dorsal tooth and cephalic projections, at least for some of these ants. But could the impalement of prey be possible for all of these ants? Extant ants and other predatory insects have evolved a marvelous diversity of mandibular forms for dealing with diverse resources, but prey capture in all is associated with robust mandibular teeth and/or setae. Even in the case of relatively slender teeth, they are acutely pointed (e.g., *Thaumatomyrmex* Mayr or *Strumigenys* Smith) with a round cross-section and are stout enough to penetrate and grasp prey. Extant trap jaw ants, as reviewed by Larabee and Suarez (2014), have the mandibles with relatively robust teeth, either for bludgeoning, or and in the case of penetration, acutely pointed tips that curve inwards, favoring gripping of the prey. The dorsal tooth of haidomyrmecine mandibles when shut against each other generally do not form a strong structure that is usually associated with trap jaw ants, but have a more delicate appearance. They are laterally flattened and in many species, when closed, do not shut flat against each other but diverge close to the apex. In some of these ants, such as *Ceratomyrmex*, the apex of the tooth is not acutely pointed but bluntly rounded and in others, such as *H. zigrasi*, there are setae or hairs on the apex. Setae on the apex of the tooth would be subject to rapid wear or damage upon impact with prey. Such morphology seems ill-suited for the impalement of prey. Cao et al. (2020) favor a liquid diet as likely for haidomyrmecines, implying the consideration of both honeydew and hemolymph as potential food sources. Predation and honeydew foraging can be found in ant genera such as such as *Myrmecia* Fabricius and *Paraponera* Smith (Fewell et al., 1996; Shattuck, 1999) so both behaviors could have been part of haidomyrmecine natural history.

The greatly expanded clypeus of haidomyrmecine ants may have played a role in their diet. The prepharynx (= cibarium) is the sucking pump for ingesting food and the muscles responsible for the sucking are attached to the clypeus (Richter et al., 2019). A larger clypeus affords a larger area for muscle attachment and hence, larger and more powerful muscles for sucking (Snodgrass, 1935). Ants may lick or suck liquid food (Paul and Roces, 2003) and typically ants with a predominant liquid diet such as formicines and dolichoderines will bear a much larger clypeus than in predatory ants (Keller, 2009). Perhaps the cephalic projections and trigger hairs were used for carefully placing the mandibles in a specific, constrained position, and then squeeze the resource to press it against the spicules of the setal patch to provoke exudation/bleeding. The liquid resource could have been channeled down the mandibles for subsequent suction or, if more efficient, held as a drop between the mandibles while the ant returned to the nest before further processing. Whatever the resource, it was probably a common and stable feature of the still gymnosperm-dominated flora of the Aptian-Albian or its associated fauna. Besides the fact that these ants are only known from amber, a product that favors the sampling of small arboreal invertebrates, the morphology of these ants also suggest arboreal foraging: a elongate slender body with elongate legs, well-developed eyes, a well-developed arolium, and strongly hooked claws. Perhaps some of these ants were engaged in some sort of symbiotic relation with other organisms and partially occupying the liquid-diet niche that formicines and dolichoderines now occupy. Hemiptera were already a well-established and diversified group by the time ants made their appearance (Johnson et al., 2018).

Amber of a later age (Upper Campanian, 72 my) from central Myanmar, includes ants recognizable as Dolichoderinae and Ponerinae, but no Haidomyrmecini (Zheng et al., 2018). These fossils are now from floras clearly dominated by angiosperms. Insects associated with the earlier gymnosperm-dominated floras have either become extinct, some have survived, and others adapted to new hosts (Peris et al., 2017). The radiation of modern ant lineages, such as Formicinae, may have also exerted additional competitive pressure on these extreme specialists, pushing them over the brink into extinction. The absence of haidomyrmecines in this more recent burmite suggests hell ants were in decline by this time. This scenario has been specifically proposed by Barden and Grimaldi (2016) within the context of “dynastic succession” as postulated by Wilson and Hölldobler (2005) and also favored by Borysenko (2017). If we consider the tens of millions of years between the Eocene and Miocene, a time of great ant diversification (LaPolla et al., 2013; Barden, 2017), we can only assume the presently known Cretaceous stem species are but a minute representation of a fabulous diversity that also had some tens of millions of years to evolve. Clearly there were predators, but that is just one of many possible life histories for these ants.

6. Conclusions

The species described here provide new views into ancient diversifications and morphologies. We hope to have included characters not previously considered but important for an improved understanding of stem ants and what they might mean for crown groups. The diversity of stem ants has only been superficially touched and there is no reason to believe Cretaceous ants were any less diverse, both morphologically and in their natural history, than their extant counterparts. While this has been recognized by recent authors, it is not always so easily put in practice. There is a long tradition of considering certain predatory groups with more generalized morphologies and life history traits as "primitive" (e.g., Ponerinae, Amblyoponinae, Ectatomminae). This perhaps has created a subconscious bias that makes us view "primitive" ants firstly as predators and also make us forget that the antecedent millions of years of evolutionary history to the amber instances we study have been more than enough to engender myriads of marvelous life histories. Some coinciding with those of extant ants, some analogous, and some totally different to anything we currently know.

CRediT authorship contribution statement

John E. Lattke: Writing - original draft, Writing - review & editing. **Gabriel A.R. Melo:** Conceptualization, Writing - review & editing.

Acknowledgements

The authors thank Rodrigo Feitosa, Julio Chaul, Bendon Boudinot, and Roberto Keller for stimulating discussions and critical comments that improved the manuscript. Isaac Reis Jorge digitized the line drawings. We also thank Philip Barden and Vincent Perrichot for inspiring discussions on fossil ants during the 2017 Simposio Mirmecologico in Curitiba, Brazil. V. Perrichot and an anonymous reviewer made lucid comments and corrections that vastly improved this manuscript, a true learning experience. This research received partial financial support from CNPq to GARM (grant 309641/2016-0).

References

Barden, P., 2017. Fossil ants (Hymenoptera: Formicidae): ancient diversity and the rise of modern lineages. Myrmecological News 14, 1–30. https://doi.org/10.25849/myrmecol.news_024:001.

Barden, P., Grimaldi, D., 2012. Rediscovery of the bizarre Cretaceous ant *Haidomyrmex* Dlussky (Hymenoptera: Formicidae), with two new species. American Museum Novitates 3755, 1–16.

Barden, P., Grimaldi, D., 2016. Adaptive radiation in socially advanced stem-group ants from the Cretaceous. Current Biology 26, 515–521. https://doi.org/10.1016/j.cub.2015.12.060.

Barden, P., Herhold, H.W., Grimaldi, D., 2017. A New Genus of Hell Ants from the Cretaceous (Hymenoptera: Formicidae: Haidomyrmecini) with a Novel Head Structure. Systematic Entomology 42, 837–846. https://doi.org/10.1111/syen.12253.

Beutel, R., Vilhelmsen, L., 2007. Head anatomy of Xyelidae (Hexapoda: Hymenoptera) and phylogenetic implications. Organisms, Development and Evolution 7 (3), 207–230. https://doi.org/10.1016/j.ode.2006.06.003.

Bolton, B., 2003. Synopsis and classification of Formicidae. Memoirs of the American Entomological Institute 71, 1–370.

Borysenko, L., 2017. Description of a new genus of primitive ants from Canadian amber, with the study of relationships between stem- and crown-group ants (Hymenoptera: Formicidae). Insecta Mundi 570, 1–57.

Buffington, M., 2012. Description of *Nanocthulhu lovecrafti*, a preternatural new genus and species of Trichoplastini (Figitidae: Eucoilinae). Proceedings of the Entomological Society of Washington 114 (1), 5–16. https://doi.org/10.4289/0013-8797.114.1.5.

Burks, R., Heraty, J., 2015. Subforaminal bridges in Hymenoptera (Insecta), with a focus on Chalcidoidea. Arthropod Structure and Development 44, 173–194. https://doi.org/10.1016/j.asd.2014.12.003.

Cao, H.-J., Perrichot, V., Shih, C., Ren, D., Gao, T.-P., 2020. A revision of *Haidomyrmex cerberus* Dlussky (Hymenoptera: Formicidae: Sphecomyrminae) from mid-Cretaceous Burmese amber. Cretaceous Research 106, 104226. https://doi.org/10.1016/j.cretres.2019.104226.

Dlussky, G.M., 1996. Ants (Hymenoptera: Formicidae) from Burmese amber. Paleontological Journal 30, 449–454.

Dong, F., Shih, C., Ren, D., 2015. A new genus of Tanyderidae (Insecta: Diptera) from Myanmar amber, Upper Cretaceous. Cretaceous Research 54, 260–265. https://doi.org/10.1016/j.cretres.2014.12.011.

Fewell, J., Harrison, J., Lighton, J., Breed, M., 1996. Foraging energetics of the ant, *Paraponera clavata*. Oecologia 105, 419–427. https://doi.org/10.1007/BF00330003.

Harris, R.A., 1979. A glossary of surface sculpturing, vol. 28. California Department of Food and Agriculture, Bureau of Entomology, pp. 1–31.

Johnson, K., Dietrich, C., Friedrich, F., Beutel, R., Wipfler, B., Peters, R., Allen, J., Petersen, M., Donath, A., Walden, K., Kozlov, A., Podsiadlowski, L., Mayer, C., Meusemann, K., Vasilikopoulos, A., Waterhouse, R., Cameron, S., Weirauch, C., Swanson, D., Percy, D., Hardy, N., Terry, I., Liu, S., Zhou, X., Misof, B., Robertson, H., Yoshizawa, K., 2018. Phylogenomics and the evolution of hemipteroid insects. Proceedings of the National Academy of Sciences USA 115 (50), 12775–12780. https://doi.org/10.1073/pnas.1815820115.

Keller, R., 2009. Homology Weekly: Clypeus. Archetype. Ant reconstruction one homology at a time. Consulted on 20.VI.2019. http://blog-rkp.kellerperez.com/2009/05/homology-weekly-clypeus.

Keller, R., 2011. A phylogenetic analysis of ant morphology (Hymenoptera: Formicidae) with special reference to the poneromorph subfamilies. Bulletin of the American Museum of Natural History 355, 1–90.

Keller, R., Hita-García, F., Economo, E., 2019. Mandibular Report: 3D comparative anatomy informs the evolution of ant mandibles as multipurpose tools. (p. 44). In: Solar, R. (Ed.), Abstract Book. XXIV Simpósio de Mirmecologia, Universidade Federal de Minas Gerais, Universidade Federal de Viçosa. Belo Horizonte, Brazil, p. 369.

LaPolla, J.S., Dlussky, G.M., Perrichot, V., 2013. Ants and the Fossil Record. Annual Review of Entomology 58, 609–630. https://doi.org/10.1146/annurev-ento-120710-100600.

Larabee, F.J., Suarez, A., 2014. The evolution and functional morphology of trap-jaw ants (Hymenoptera: Formicidae). Myrmecological News 20, 25–36.

Latreille, P.A., 1809. Genera crustaceorum et insectorum secundum ordinem naturalem in familias disposita, iconibus exemplisque plurimus explicata. Tomus 4.. Parisiis et Argentorati [= Paris and Strasbourg]: A. Koenig.

Lattke, J., Delsinne, T., Alpert, G., Guerrero, R., 2018. Ants of the genus *Protalaridris*, more than just deadly mandibles. European Journal of Entomology 115, 269–295. https://doi.org/10.14411/eje.2018.027.

Masner, L., Johnson, N.F., Arias-Penna, T.M., 2007. *Tyrannoscelio*, a new genus of Neotropical Scelionidae (Hymenoptera: Platygastroidea) with description of two new species. American Museum Novitates 3551, 8. http://hdl.handle.net/2246/5838.

McKellar, R., Glasier, J., Engel, M., 2013. A new trap-jawed ant (Hymenoptera: Formicidae: Haidomyrmecini) from Canadian Late Cretaceous amber. The Canadian Entomologist 145, 454–465. https://doi.org/10.4039/tce.2013.23.

Miao, Z., Wang, M., 2019. A new species of hell ants (Hymenoptera: Formicidae: Haidomyrmecini) from the Cretaceous Burmese amber. Journal of the Guangxi Normal University 37, 139–142 (Natural Science Edition).

Nielsen, M., Buffington, M., 2011. Redescription of *Stentorceps* Quinlan, 1984 (Hymenoptera: Figitidae), with a description of five new species. African Entomology 19 (3), 597–614.

Paul, J., Roces, F., 2003. Fluid intake rates in ants correlate with their feeding habits. Journal of Insect Physiology 49 (2003), 347–357.

Peris, D., Labandeira, C., Peñalver, E., Delclòs, X., Barrón, E., Pérez-de la Fuente, R., 2017. The case of *Darwinylus marcosi* (Insecta: Coleoptera: Oedemeridae): A Cretaceous shift from a gymnosperm to an angiosperm pollinator mutualism. Communicative & Integrative Biology 10, 4. https://doi.org/10.1080/19420889.2017.1325048 e1325048.

Perrichot, V., Nel, A., Neraudeau, D., Lacau, S., Guyot, T., 2008. New fossil ants in French Cretaceous amber (Hymenoptera: Formicidae). Naturwissenschaften 95, 91–97. https://doi.org/10.1007/s00114-007-0302-7.

Perrichot, V., Wang, B., Engel, M., 2016. Extreme morphogenesis and ecological specialization among Cretaceous basal ants. Current Biology 26, 1468–1472. https://doi.org/10.1016/j.cub.2016.03.075.

Perrichot, V., Wang, B., Barden, P., 2020. New remarkable hell ants (Formicidae: Haidomyrmecinae stat. nov.) from mid-Cretaceous amber of northern Myanmar. Cretaceous Research 109, 104381. https://doi.org/10.1016/j.cretres.2020.104381.

Richter, A., Keller, R., Baumgarten Rosumek, F., Economo, E., Hita Garcia, F., Beutel, R., 2019. The cephalic anatomy of workers of the ant species *Wasmannia affinis* (Formicidae, Hymenoptera, Insecta) and its evolutionary implications. Arthropod Structure & Development 49, 26–49. https://doi.org/10.1016/j.asd.2019.02.002.

Shattuck, S.O., 1999. Australian ants. Their biology and identification. CSIRO Publishing, Collingwood, Victoria xi + 226 pp.

Shi, G., Grimaldi, D., Harlow, G., Wang, J., Wang, J., Yand, M., Lei, W., Li, Q., Li, X., 2012. Age constraint on Burmese amber based on U-Pb dating of zircons. Cretaceous Research 37, 155–163. https://doi.org/10.1016/j.cretres.2012.03.014.

Snodgrass, R.E., 1935. Principles of insect morphology. McGrawHill, New York, p. 667 pp.

Wang, W., Lin, L., Xiang, X., Ortiz, R., Liu, Y., Xiang, K., Yu, S., Xing, Y., Chen, Z., 2016. The rise of angiosperm- dominated herbaceous floras: Insights from Ranunculaceae. Scientific Reports 6, 27259. https://doi.org/10.1038/srep27259.

Wilson, E.O., 1955. A monographic revision of the ant genus *Lasius*. Bulletin of the Museum of Comparative Zoology 113, 1–201.

Wilson, E.O., Brown Jr., W.L., 1967. [Untitled. Descriptions of new taxa: Sphecomyrminae Wilson and Brown, new subfamily; *Sphecomyrma* Wilson and Brown, new genus; *Sphecomyrma freyi* Wilson and Brown, new species.]. Pp. 6-10 in: Wilson, E. O.; Carpenter, F. M.; Brown, W. L., Jr. 1967. The first Mesozoic ants, with the description of a new subfamily. Psyche 74, 1–19.

Wilson, E.O., Hoelldobler, B., 2005. The rise of the ants: a phylogenetic and ecological explanation. Proceedings of the National Academy of Sciences USA 102, 7411–7414. https://doi.org/10.1073/pnas.0502264102.

Zheng, D., Chang, S.-C., Perrichot, V., Dutta, S., Rudra, A., Mu, L., Kelly, R., Li, S., Zhang, Q., Wong, J., Wang, J., Wang, H., Fang, F., Zhang, H., Wang, B., 2018. A Late Cretaceous amber biota from central Myanmar. Nature Communications 9, 3170. https://doi.org/10.1038/s41467-018-05650-2.